

Theory of High Harmonic Generation for Probing Time-Resolved Large-Amplitude Molecular Vibrations with Ultrashort Intense Lasers

Anh-Thu Le,¹ T. Morishita,² R. R. Lucchese,³ and C. D. Lin¹

¹*Department of Physics, Cardwell Hall, Kansas State University, Manhattan, Kansas 66506, USA*

²*Department of Engineering Science, University of Electro-Communications, 1-5-1 Chofu-ga-oka, Chofu-shi, Tokyo 182-8585, Japan*

³*Department of Chemistry, Texas A&M University, College Station, Texas 77843-3255, USA*

(Received 29 February 2012; published 14 November 2012)

We present a theory that incorporates the vibrational degrees of freedom in a high-order harmonic generation (HHG) process with ultrashort intense laser pulses. In this model, laser-induced time-dependent transition dipoles for each fixed molecular geometry are added coherently, weighted by the laser-driven time-dependent nuclear wave packet distribution. We show that the nuclear distribution can be strongly modified by the HHG driving laser. The validity of this model is first checked against results from the numerical solution of the time-dependent Schrödinger equation for a simple model system. We show that in combination with the established quantitative rescattering theory this model is able to reproduce the time-resolved pump-probe HHG spectra of N₂O₄ reported by Li *et al.* [Science **322**, 1207 (2008)].

DOI: [10.1103/PhysRevLett.109.203004](https://doi.org/10.1103/PhysRevLett.109.203004)

PACS numbers: 33.80.Eh, 42.65.Ky

High-order harmonic generation (HHG) has attracted a great deal of attention over the past two decades for its application as a tabletop coherent extreme ultraviolet source [1,2] and as a source of attosecond pulses [3,4]. In recent years, it has been shown that HHG signals also encode information about the target [5–8]. Since driving laser pulses as short as a few femtoseconds are available, HHG spectroscopy has been perceived as a possible tool for probing chemical processes that evolve in few-femtosecond time scales. Indeed a few pioneering pump-probe experiments have been performed so far on different targets, e.g., SF₆ [9], N₂O₄ [10], Br₂ [11,12], and NO₂ [13], where a dynamic system is initiated either by IR light or its second harmonics, and the time evolution of the system is probed by observing the high harmonics generated by another IR light at varying time delays. Unfortunately, with no accurate theories available, these experiments have been interpreted in terms of simple models, thus leaving out many interesting reaction dynamics buried in the measured data.

HHG is a nonlinear process. It is not easily amendable to full *ab initio* calculations, especially for polyatomic molecules. There have been several attempts to include the nuclear degrees of freedom in HHG theory [14–20]. They are based on simplified models or direct solution of time-dependent Schrödinger equation (TDSE) for simple systems. Most of the models have not been fully calibrated; thus, their validity is not known. While there has been some success, for example, the prediction [14] of isotope effect in HHG and its experimental confirmation [21], on the whole, it is fair to say that there still exists no reliable theoretical tool for calculating HHG spectra from a time-evolving molecular system. In fact, even within the fixed-nuclei approximation, there are few reliable calculations of HHG from molecules.

The goal of this Letter is twofold. First, we develop a general theory for HHG which includes the vibrational degrees of freedom; see Eqs. (1) and (2) below. Second, as an application we combine this theory with the recently developed quantitative rescattering (QRS) theory [7,8] to calculate HHG from vibrating N₂O₄, which was the subject of a recent experiment by Li *et al.* [10]. Developed initially for the case of fixed nuclei, the QRS is computationally efficient and has been well tested [22,23]. Furthermore, with the inclusion of macroscopic propagation effect [24–26], the predicted HHG spectra based on QRS have been shown to agree well with experiments for different molecules.

We consider a homonuclear diatomic molecule in the electronic ground state under a few-cycle intense laser pulse. We will show below that the induced dipole $\bar{D}(t)$ can be calculated as

$$\bar{D}(t) = \int dR |\chi(R, t)|^2 D(t; R), \quad (1)$$

where $\chi(R, t)$ is the nuclear wave function and $D(t; R)$ is the induced dipole from a molecule with a fixed internuclear distance R . In practice, one can also use the dipole acceleration form in Eq. (1). The HHG power spectrum is related to the induced dipole in frequency domain $\bar{D}(\Omega)$ by $S(\Omega) \sim |\bar{D}(\Omega)|^2$.

It is important to emphasize that the *real* meaning of $\chi(R, t)$ has not been specified. In fact, Eq. (1) has been used before by some authors, for example, in Ref. [19], but $\chi(R, t)$ was assumed to be unmodified under the influence of the HHG driving laser. In this Letter we show that $\chi(R, t)$ can be significantly modified due to the HHG driving laser and is the solution of the Schrödinger equation (in atomic units)

$$i \frac{\partial \chi(R, t)}{\partial t} = \left[-\frac{1}{2\mu} \frac{\partial^2}{\partial R^2} + U(R) - \frac{1}{2} \sum_{ij} \alpha_{ij}(R) E_i(t) E_j(t) \right] \chi(R, t), \quad (2)$$

where μ is the reduced mass, $U(R)$ is the potential energy surface, α_{ij} is the polarizability tensor, and $E_i(t)$ is the component of the electric field of the laser along the i axis. We only consider the cases when laser intensity is well below the target saturation intensity so that the depletion of the ground state is negligible. In those cases, the contribution from higher order terms (involving hyperpolarizabilities) in Eq. (2) is insignificant. Analogous to the Born-Oppenheimer (BO) approximation, Eq. (2) describes the nuclear motion in the field-dressed picture, where the nuclei couple with the laser through the induced polarization. Our approach can be thought of as an extension of the BO approximation to the time-dependent case, applied for a HHG process. A more general formulation within the BO expansion has been discussed recently [27,28], but there have been no numerical applications thus far. Equation (2) has been used to treat stimulated Raman scattering process [29]. In connection with HHG, an attempt to use this equation has been reported before for the case of small vibrational amplitude [16]; however, the validity of the model has not been reported. We comment that our approach also differs from the model proposed by Lein [14], in which the dynamic change of the nuclear wave function of the parent ion between ionization and recombination steps is taken into account, but the vibrational nuclear wave function is assumed to be time independent; see Eq. (4) of Ref. [14].

To validate the model described by Eqs. (1) and (2), we apply it to a collinear mass-scaled H_2^+ , in which the electron and nuclei are restricted to move along the laser polarization direction [30–32]. We compare predictions of the model (denoted in the following as “model”) against the accurate numerical solution of the TDSE for the same system (denoted as “exact”). In the model, the induced dipole $D(t; R)$ for a fixed R is calculated from the numerical solution of the 1D TDSE with frozen nuclei, and the nuclear wave function $\chi(R, t)$ is obtained by solving Eq. (2). In the calculation, we use an 8-cycle, sine-squared envelope laser pulse of 800 nm wavelength with an intensity of 2.5×10^{14} W/cm².

First we show in Fig. 1(a) HHG spectrum from the initial $v = 0$ vibrational state (in the ground electronic state) for a “hydrogen” mass of $4M_p$ (M_p being the mass of a proton), calculated with exact and model. Clearly, the two results are almost identical. Similar good agreements between the two methods are also found for other vibrational states (see the Supplemental Material [33]). We do note a significant deviation in the spectrum in the model calculation if the nuclear wave function is assumed to be unmodified by the laser (thin blue line). This indicates that the laser field can

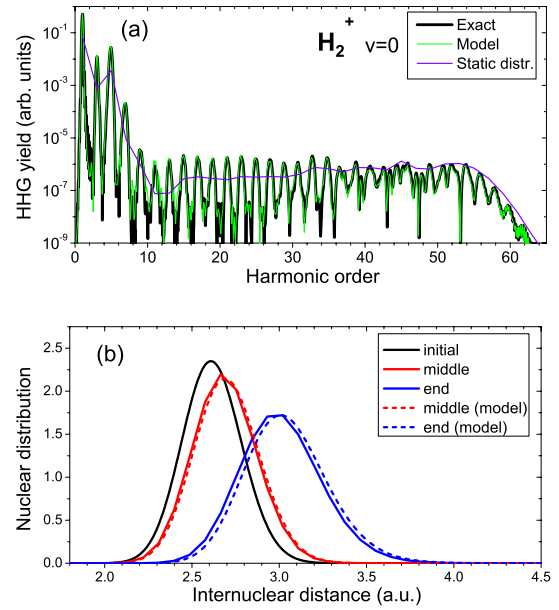


FIG. 1 (color online). (a) HHG spectrum from $v = 0$ vibrational state of hydrogenlike H_2^+ with the hydrogen atom mass of $4M_p$, calculated by the exact TDSE and the model. Spectrum calculated with a static nuclear distribution is also shown (thin blue line, only odd harmonics are shown). (b) Nuclear distributions at the beginning, the middle, and the end of the laser pulse calculated by the exact TDSE and by using Eq. (2).

influence nuclear dynamics and modify the HHG spectrum. From the TDSE results, one can follow the evolution of the nuclear distribution, as shown in Fig. 1(b), at the beginning, the middle, and the end of the laser pulse. They agree well with those calculated from Eq. (2) (dashed lines). We have also verified that the one-channel model is adequate as the population in the σ_u dissociative potential curve is practically nil after the pulse is over.

Next we test the case when the initial state is a nuclear wave packet. We choose the initial wave function at time $t_0 = 0$ to be a linear combination of $v = 0, 1$, and 2 vibrational states with the coefficients of $0.8, 0.5$, and 0.332 , respectively. The mass of hydrogen is chosen to be $16M_p$. We found that the HHG spectra for any fixed time delay between t_0 and the beginning of the probe laser pulse, calculated by the exact and model, are nearly indistinguishable [33]. The HHG yields are found to modulate as a function of time delay with a period of $T = 64$ fs, equal to the vibrational period of this mass-scaled H_2^+ . For comparison, we show in Figs. 2(a) and 2(b) HHG yields for a few harmonics as a function of time delay. Again, we note an overall very good agreement between the two methods. More detailed analysis reveals that the peak near the time delay of $0.9 T$ is associated with the nuclei distributed at the peak of the pulse at large R where the HHG process is more efficient due to a smaller ionization potential.

An advantage of the present approach is that Eqs. (1) and (2) can be readily used in combination with the QRS theory

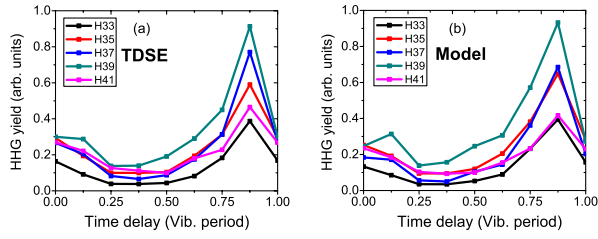


FIG. 2 (color online). HHG yields for a few different harmonics versus time delay from the TDSE (a) and the model using Eqs. (1) and (2) (b) for a case of a nuclear wave packet. The hydrogen atom mass is $16M_p$.

[7,8,22,23], which has been well tested for the case of frozen nuclei. As a practical application we consider the vibrating N_2O_4 studied by Li *et al.* [10], where a vibrational nuclear wave packet was first initiated by a short laser pulse (the pump) with a relative weak intensity of $2 \times 10^{13} \text{ W/cm}^2$. This excitation is understood as an impulsive stimulated Raman scattering [9,29,34]. High-order harmonics were then generated with a more intense pulse at an intensity of $2 \times 10^{14} \text{ W/cm}^2$ (the probe), with some time delay with respect to the pump pulse. Both pulses were of 800 nm wavelength and 30 fs duration (FWHM). The measured HHG yield was found to modulate as a function of time delay with a period identical to the vibrational period of the symmetric stretch mode. Since the N-N symmetric stretch is most dominant in this excitation scheme, it is reasonable to approximate the changes in N_2O_4 as due to the change in the N-N distance, R_{NN} . In our simulation, the nuclear wave packet initiated by the pump pulse is calculated from Eq. (2), in which N_2O_4 is modeled as an effective diatomic molecule. This wave packet is subsequently modified during the probe pulse, which is also simulated by solving Eq. (2). We used MOLPRO [35] to calculate electronic and molecular structure. Photoionization cross sections for each fixed geometry were calculated with the state-of-the-art molecular photoionization code [36]. We limit ourselves to parallel pump and probe laser polarizations only. For simplicity we further assume that all molecules are aligned with the N-N axis along the laser polarization direction. To minimize the ionization depletion effect in our simulation, a probe pulse of duration 20 fs and intensity of $1.5 \times 10^{14} \text{ W/cm}^2$ is used.

Photoionization (differential) cross sections as a function of R_{NN} near the equilibrium distance $R_{NN} = 1.8 \text{ \AA}$ are presented in Fig. 3(a) for energies corresponding to harmonic orders 17 (H17), 21 (H21), and 25 (H25). These cross sections, together with the transition dipole phases, are used in the QRS to obtain induced dipole $D(r; R)$ for each R . We note significant differences between these results and that of Li *et al.* [10], where the eikonal-Volkov approximation was used to calculate these quantities. The harmonic yields as functions of R_{NN} calculated

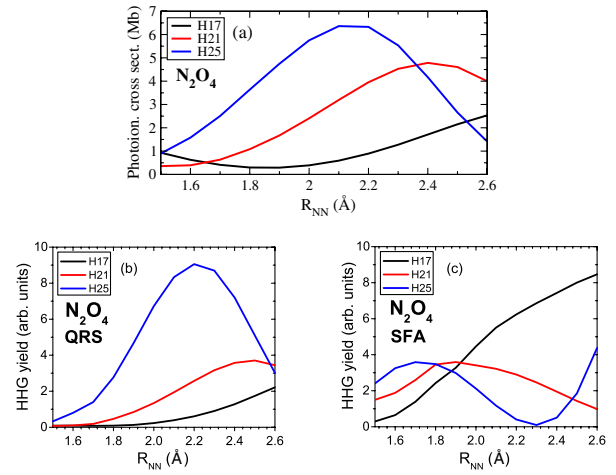


FIG. 3 (color online). (a) Photoionization cross section for a few different energies corresponding to H17, H21, and H25. (b),(c) HHG yields from N_2O_4 versus R_{NN} from the QRS and SFA, respectively.

with the QRS, as shown in Fig. 3(b), closely resemble the photoionization cross sections shown in Fig. 3(a). This is at variance with the results from the strong-field approximation (SFA) [37], shown in Fig. 3(c), which exhibit a nonmonotonic behavior for higher harmonic orders. Furthermore, comparing to Li *et al.* [10], where the two highest occupied molecular orbitals (HOMO and HOMO-1) were claimed to contribute to ionization, our calculations using the strong-field approximation and molecular tunneling ionization theory [38] both show an insignificant ionization leading to the B_{2g} cation state, in agreement with a recent calculation [20].

Next we carry out calculations on N_2O_4 using our model [Eqs. (1) and (2)], with the input for fixed-nuclei-induced dipoles $D(r; R)$ from QRS and SFA. For simplicity, in the following we refer to these two calculations as model + QRS (or simply QRS) and model + SFA (or simply SFA). The key results are shown in Fig. 4 and summarized here. (i) Modulation of HHG signal for all harmonics with a period of about 125 fs, which is the vibrational period of the symmetric-stretch mode in N_2O_4 ($T \approx 130 \text{ fs}$). HHG yields for a few harmonics as functions of time delay between pump and probe pulses, calculated with model + QRS and model + SFA, are shown in Figs. 4(a) and 4(b), respectively. The results have been normalized to those without the pump pulse. (ii) The magnitude of the modulation is about 80% (40%) for the QRS (SFA), which is about a factor of 4 (2) larger than the experiment. This is due to the fact that all the molecules were assumed to be perfectly aligned along the pump laser polarization direction. Since the impulsive stimulated Raman scattering process is less efficient if the molecule is not aligned along the laser, averaging over the molecular alignment would reduce the modulation depth. (iii) The modulation depth decreases with harmonic order, and all the harmonic orders

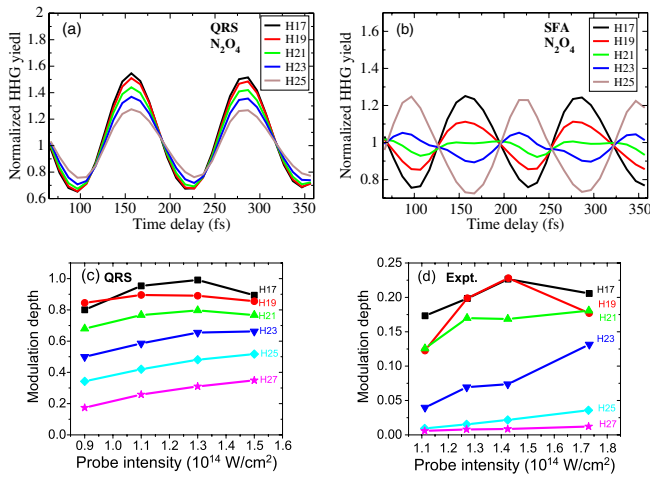


FIG. 4 (color online). Normalized HHG yields from N_2O_4 versus pump-probe time delay for a few different harmonics from the model + QRS (a) and the model + SFA (b). Probe laser intensity dependence of the modulation depth from the model + QRS (c) and the JILA experiment [10] (d). Molecules are assumed to be perfectly aligned along the pump laser polarization direction.

from H17 to H25 are in phase, in agreement with the experiment. It is not so for the SFA results. We further comment that the recent calculation based on the coupled time-dependent single-particle Schrödinger equation by Spanner *et al.* [20] does not agree with the experiment. (iv) The first peak occurs at a time delay of 160 fs, in good agreement with the experimental value of 170 ± 10 fs. (v) The maximum (minimum) HHG yield corresponds to the time delay when the nuclei are mostly distributed at larger (smaller) R_{NN} at the peak of the probe pulse [33]. This is found in the experiment and in the QRS, but not in the SFA calculation. We emphasize once again that the dynamic of the N_2O_4 nuclear wave packet during the probe pulse is strongly modified by the laser [33]. This fact was not addressed in Li *et al.* [10] nor in most theoretical consideration so far. (vi) The QRS predicts that the modulation depth increases slightly with the probe laser intensity, see Fig. 4(c), in agreement with the experiment, see Fig. 4(d). This is probably due to the fact that at a higher intensity, the nuclear wave packet extends during the probe to a larger R , where the HHG process is more efficient.

In conclusion, we have developed an efficient method to calculate high-order harmonics generated from dynamically evolving molecular systems. By combining this method with the QRS we have successfully explained many features of the observed high harmonic spectra from vibrating N_2O_4 molecules reported in Li *et al.* [10]. One important result of this work is that the vibrational wave packet is modified by the probing laser, which has been neglected in all previous models used in the interpretation of experimental data so far [9–12]. The present approach thus has provided the needed framework to

disentangle electron-nuclear coupling dynamics in the HHG process, in which practical simulations for HHG from evolving targets can be carried out. We suggest that further experiments on N_2O_4 molecules be carried out, in particular, to use a second pump laser to further excite the nuclear wave packet generated by the first pump, at different time delay. By proper timing, larger vibrational amplitudes can be achieved, and the nuclear wave packet can be similarly probed with HHG. Such experiments can deliver a wealth of data to test the prediction of the present model and to provide a more complete picture of this system. To provide realistic theoretical simulations for the experiments on Br_2 and NO_2 mentioned earlier, however, the present model has to be extended to include multiple electronic surfaces. In connection with the possibility of extracting target structure by using HHG, our results indicate that because of strong nature of the probe pulse, the probed nuclear distribution does, in general, change itself significantly due to the interaction with the probe. Therefore, an inversion procedure to obtain the “original” nuclear distribution should be more involved than one would expect in the case of a perturbative probe. We note that this is relevant not only to HHG, but to any nonlinear strong-field process involving molecular targets, such as ionization, above-threshold ionization, and nonsequential double ionization. The effect is general, but it is stronger for molecules that are more sensitive to Raman scattering.

This work was supported in part by the Chemical Sciences, Geosciences and Biosciences Division, Office of Basic Energy Sciences, Office of Science, U.S. Department of Energy.

-
- [1] F. Krausz and M. Ivanov, *Rev. Mod. Phys.* **81**, 163 (2009).
 - [2] T. Popmintchev, M. C. Chen, P. Arpin, M. M. Murnane, and H. C. Kapteyn, *Nature Photon.* **4**, 822 (2010).
 - [3] G. Sansone *et al.*, *Science* **314**, 443 (2006).
 - [4] R. Lopez-Martens *et al.*, *Phys. Rev. Lett.* **94**, 033001 (2005).
 - [5] J. Itatani, J. Levesque, D. Zeidler, H. Niikura, H. Pepen, J. C. Kiefer, P. B. Corkum, and D. M. Villeneuve, *Nature (London)* **432**, 867 (2004).
 - [6] M. Lein, *J. Phys. B* **40**, R135 (2007).
 - [7] T. Morishita, A. T. Le, Z. Chen, and C. D. Lin, *Phys. Rev. Lett.* **100**, 013903 (2008).
 - [8] A. T. Le, R. R. Lucchese, M. T. Lee, and C. D. Lin, *Phys. Rev. Lett.* **102**, 203001 (2009).
 - [9] N. L. Wagner, A. Wüest, I. P. Christov, T. Popmintchev, X. Zhou, M. M. Murnane, and H. C. Kapteyn, *Proc. Natl. Acad. Sci. U.S.A.* **103**, 13 279 (2006).
 - [10] W. Li, X. Zhou, R. Lock, S. Patchkovskii, A. Stolow, H. C. Kapteyn, and M. M. Murnane, *Science* **322**, 1207 (2008).
 - [11] H. J. Wörner, J. B. Bertrand, D. V. Kartashov, P. B. Corkum, and D. M. Villeneuve, *Nature (London)* **466**, 604 (2010).
 - [12] H. J. Wörner, J. B. Bertrand, P. B. Corkum, and D. M. Villeneuve, *Phys. Rev. Lett.* **105**, 103002 (2010).

- [13] H. J. Wörner, J. B. Bertrand, B. Fabre, J. Higuët, H. Ruf, A. Dubrouil, S. Patchkovskii, M. Spanner, Y. Mairesse, V. Blanchet, E. Mevel, E. Constant, P. B. Corkum, and D. M. Villeneuve, *Science* **334**, 208 (2011).
- [14] M. Lein, *Phys. Rev. Lett.* **94**, 053004 (2005).
- [15] C. B. Madsen and L. B. Madsen, *Phys. Rev. A* **74**, 023403 (2006).
- [16] Z. B. Walters, S. Tonzani, and C. H. Greene, *J. Phys. B* **40**, F277 (2007).
- [17] P. P. Corso, E. Fiordilino, and F. Persico, *J. Phys. B* **40**, 1383 (2007).
- [18] C. C. Chirila and M. Lein, *Phys. Rev. A* **77**, 043403 (2008).
- [19] M. Y. Emelin, M. Y. Ryabikin, and A. M. Sergeev, *New J. Phys.* **10**, 025026 (2008).
- [20] M. Spanner, J. Mikosch, A. E. Boguslavskiy, M. M. Murnane, A. Stolow, and S. Patchkovskii, *Phys. Rev. A* **85**, 033426 (2012).
- [21] S. Baker, J. S. Robinson, C. A. Haworth, H. Teng, R. A. Smith, C. C. Chirilă, M. Lein, J. W. G. Tisch, and J. P. Marangos, *Science* **312**, 424 (2006).
- [22] A. T. Le, R. R. Lucchese, S. Tonzani, T. Morishita, and C. D. Lin, *Phys. Rev. A* **80**, 013401 (2009).
- [23] C. D. Lin, A. T. Le, Z. Chen, T. Morishita, and R. R. Lucchese, *J. Phys. B* **43**, 122001 (2010).
- [24] C. Jin, A. T. Le, and C. D. Lin, *Phys. Rev. A* **79**, 053413 (2009).
- [25] C. Jin, H. J. Wörner, V. Tosa, A. T. Le, J. B. Bertrand, R. R. Lucchese, P. B. Corkum, D. M. Villeneuve, and C. D. Lin, *J. Phys. B* **44**, 095601 (2011).
- [26] C. Jin, J. B. Bertrand, R. R. Lucchese, H. J. Wörner, P. B. Corkum, D. M. Villeneuve, A. T. Le, and C. D. Lin, *Phys. Rev. A* **85**, 013405 (2012).
- [27] L. S. Cederbaum, *J. Chem. Phys.* **128**, 124101 (2008).
- [28] A. Abedi, N. T. Maitra, and E. K. U. Gross, *Phys. Rev. Lett.* **105**, 123002 (2010).
- [29] L. Dhar, J. A. Rogers, and K. A. Nelson, *Chem. Rev.* **94**, 157 (1994).
- [30] K. C. Kulander, F. H. Mies, and K. J. Schafer, *Phys. Rev. A* **53**, 2562 (1996).
- [31] W. Qu, Z. Chen, Z. Xu, and C. H. Keitel, *Phys. Rev. A* **65**, 013402 (2001).
- [32] N. Takemoto and A. Becker, *Phys. Rev. Lett.* **105**, 203004 (2010).
- [33] See Supplemental Material at <http://link.aps.org/supplemental/10.1103/PhysRevLett.109.203004> for (i) comparison of HHG spectra from exact TDSE and the model for initial $v = 1$ and $v = 2$ vibrational states as well as an initial state as a wave packet for mass-scaled H_2^+ and (ii) evolution of the N_2O_4 nuclear wave packet during the pump and probe laser pulses.
- [34] R. A. Bartels, T. C. Weinacht, S. R. Leone, H. C. Kapteyn, and M. M. Murnane, *Phys. Rev. Lett.* **88**, 033001 (2002).
- [35] H.-J. Werner, P. J. Knowles, R. Lindh, M. Schutz, P. Celani, T. Korona, F. R. Manby, G. Rauhut, R. D. Amos, A. Bernhardsson, A. Berning, D. L. Cooper, M. J. O. Deegan, A. J. Dobbyn, F. Eckert, C. Hampel, G. Hetzer, A. W. Lloyd, S. J. McNicholas, W. Meyer, M. E. Mura, A. Nicklass, P. Palmieri, R. Pitzer, U. Schumann, H. Stoll, A. J. Stone, R. Tarroni, and T. Thorsteinsson, *MOLPRO, Version 2002.6, A Package of Ab Initio Programs* (Birmingham, England, 2003).
- [36] A. P. P. Natalense and R. R. Lucchese, *J. Chem. Phys.* **111**, 5344 (1999).
- [37] M. Lewenstein, Ph. Balcou, M. Y. Ivanov, A. L'Huillier, and P. B. Corkum, *Phys. Rev. A* **49**, 2117 (1994).
- [38] X. M. Tong, Z. X. Zhao, and C. D. Lin, *Phys. Rev. A* **66**, 033402 (2002).